Çanakkale Onsekiz Mart University

Journal of Advanced Research in Natural and Applied Sciences

dergipark.org.tr/tr/pub/jarnas

Open Access

e-ISSN: 2757-5195 2024, Vol. 10, Issue 4, Pages: 786-802 doi.org/10.28979/jarnas.1516154

Theoretical Calculations and Molecular Docking Analysis of 4-(2-(4-Bromophenyl)Hydrazineylidene)-3,5-Diphenyl-4H-Pyrazole Molecule

Kenan Gören[1], Mehmet Bağlan[2], Veysel Tahiroğlu[3], Ümit Yıldıko[4]

[1,2]Department of Chemistry, Faculty of Art and Science, Kafkas University, Kars, Türkiye
[3]Department of Nursing, Faculty of Health Science, Şırnak University, Şırnak, Country
[4]Department of Bioengineering, Engineering of Architecture Faculty, Kafkas University, Kars, Türkiye

Article Info
Received: 14 Jul 2024
Accepted: 07 Oct 2024
Published: 31 Dec 2024
Research Article

Abstract − The molecular structure of 4-(2-(4-bromophenyl)hydrazineylidene)-3,5-diphenyl-4h-pyrazole (BHDH) molecule, which is a pyrazole derivative, was investigated theoretically using the Gaussian 09 program according to the Moller-Plesset (MP2) method. The MP2 method was optimized for these theoretical calculations using DGDZVP and 6-311G(d,p) basis sets. By taking geometric structures, Highest-Energy Molecular Orbital (HOMO) and Lowest-Energy Molecular Orbital (LUMO) analysis, Mulliken Atomic Charges, Molecular Electrostatic Potential (MEPS), Nonlinear Optical (NLO) features, and Natural Bond Orbital (NBO) images of the molecule from this optimized structure were analyzed. In the continuation of the study, Absorbed, Distributed, Metabolized, and Excreted (ADME) analysis was performed to evaluate the BHDH molecule as a drug. Many possible drugs for treating various medical diseases have taken their place in the world market. Drug interactions involve combinations with drugs or other substances that change the effect of a drug on the body. Molecular docking analysis of BHDH molecule on obesity disease was performed with acetylcholinesterase (AChE) and butyrylcholinesterase (BChE) enzymes. The highest binding energies and binding conformations between ligands and enzymes were predicted.

Keywords − *AChE, BChE, molecular docking, ADME, NBO*

1. Introduction

The beneficial biological functions of pyrazole compounds, an important family of heterocyclic compounds, include antidepressant, antipyretic, antibacterial, anti-inflammatory, analgesic, herbicidal, and insecticidal effects. These properties make them excellent targets for synthetic chemists [1]. Furthermore, the commercial sale of certain compounds possessing the pyrazole structure has increased interest in pharmaceutical and synthetic organic chemistry for pyrazole compounds' production and the study of their bioactive characteristics. For instance, fipronil is frequently used as an insecticide, zaleplon is used to treat insomnia, crizotinib is used to treat cancer, and penflufen is used because it has an antifungal impact [2]. Pyrazole derivatives are also utilized in pharmaceutical, agricultural, electronics, and other areas. It works well in a variety of contexts. It is employed in many fields, including medication creation and as an insecticide and pesticide in agriculture [3]. It is employed for optical qualities in the technology and pharmaceutical sectors, among other industrial domains. Polymers with pyrazole groups, for instance, are utilized in optoelectronic tools like light-releasing diodes and transistors because of their narrow band gaps. It is beneficial for gadgets [4].

[1]kenangoren49@gmail.com; (Corresponding Author) [2]mehmehbaglan36@gmail.com; [3]veysel0793@hotmail.com; [4]yildiko1@gmail.com

Globally, the frequency of overweight or obesity in children has grown, and this poses a serious public health emergency with financial ramifications and high medical expenses. Additionally, there is a correlation between juvenile obesity and a higher prevalence of comorbidities such as insulin [5]. Increased direct and indirect expenditures result from cardiovascular disease, diabetes, hypertension, resistance, and sleep apnea. The non-communicable diseases (NCD) Risk Factor Collaboration recently combined and examined population-based data on global patterns of childhood obesity [6]. It was shown that while childhood's high rates and teenage obesity continued in several Asian nations, rises in children and adolescents' body mass index stayed steady in high-income countries between 1975 and 2016. Furthermore, these inclinations have nothing to do with adult impulses anymore. Due to these factors, it is imperative that childhood obesity be prevented by detecting obese children at a young age so that successful intervention can start [7]. Children and teenagers with obesity have adipose tissue that secretes a lot of adipocytokines in addition to storing fat. Overproduction of adipocytokines can lead to oxidative stress, elevated blood pressure, insulin resistance, and abnormal lipid metabolism [8].

The term metabolic syndrome (MetS) refers to a set of risk factors that include glucose intolerance, abdominal obesity, hypertension, and problems with lipid metabolism that are linked to cardiovascular disease and type II diabetes. The persistent obesity pandemic in children and adolescents has made MetS a public health issue in this demographic as well. For improved public health, biomarkers that can forecast adolescent or pediatric populations' risk of developing metabolic syndrome are essential [9]. Handling this syndrome Acetylcholine and other choline esters are hydrolyzed by a class of enzymes that includes cholinesterase (ChE). Human tissues contain two distinct forms of ChE enzymes: acetylcholinesterase (AChE) and butyrylcholinesterase (BChE). AChE is located in the erythrocyte membrane of the skeletal muscles and central nervous system, while BChE, sometimes referred to as pseudocholinesterase, is produced in the liver and discharged into plasma [10]. At the cholinergic synapse, AChE's primary job is to hydrolyze acetylcholine. Although BChE's exact job in the body is unknown, it could be related to tissue development or detoxification. The phenylalanine residue in the acyl-binding pocket defines the pocket's structure, which in turn determines ChE enzymes' substrate specificity. The physiological role of BChE, located at the ChE catalyst's valley at the bottom, is still unknown; however, Numerous investigations have demonstrated its involvement in neurogenesis, cellular adhesion, myelin maintenance, and toxin scavenging [11]. Adult patients with hepatobiliary illnesses have been included in current investigations examining the activities of BChE in humans. Studies examining alterations in BChE activity in adult patients or those with MetS are few. Fewer studies have looked at the connection between obesity and plasma BChE concentrations in the general adolescent population, despite numerous researchers having found elevated levels of BChE in the plasma of people with MetS and abdominal obesity. Furthermore, it is yet unknown if raising BChE levels might help adolescents with MetS, although this topic has recently gained greater attention. While elevated BChE levels have been linked to obesity in several populations, the Chinese teenage population has not shown evidence of this connection [12].

An example of an ab-initio approach is the Moller-Plesset (MP) perturbation theory. The average interaction between electrons is the only factor considered by the Hartree-Fock wave function. On the other hand, immediate interactions among electrons must also be considered. Because electrons repel each other [13]. When the instantaneous interactions of the movements of electrons with each other are included in the wave function, it can be said that the instantaneous electron correlation is included in the wave function. This method also adds the electron correlation effect to the Hatree-Fock method. It does this using Rayleigh-Schrödinger perturbation theory. The Moller-Plesset method is generally used for second-, third-, and fourth-order calculations, symbolized by MP2, MP3, and MP4, respectively [14].

In this study, MP2 calculations of the pyrazole derivative BHDH [15] molecule were made with the Gaussian 09 program. In the continuation of this study, the drug properties of the 4-(2-(4-bromophenyl)hydrazineylidene)-3,5-diphenyl-4h-pyrazole (BHDH) molecule on obesity disease were examined by Absorbed, Distributed, Metabolized, and Excreted (ADME) analysis. In addition, molecular docking analysis of the BHDH molecule on obesity disease was performed with BChE and AChE enzymes.

2. Materials and Methods

For MP2, the BHDH molecule's theoretical analysis was performed utilizing Gaussian 09 [16] programs. First, the MP2 approach optimized the molecule's gas phase using the DGDZVP and 6-311G(d,p) basis sets. The BHDH compound's ADME analysis was conducted utilizing the online database Admetlab 2.0 (https://admetmesh.scbdd.com/). Schrödinger's Maestro Molecular Modeling platform (version 11.8) [17] was used for molecular docking analysis, and the resulting receptor was used to visualize 3D interactions. The Discovery Studio 2016 [18] program was used. The Origin 2019b 64-bit program was used to compare Mulliken loads graphically.

3. Results and Discussion

This section should provide/introduce/investigate the findings and discussion/definitions and theorems. Findings/Concepts obtained from the study should be supported in this section by figures, tables/propositions, and examples. For Results and Discussion, the similarities and differences of the obtained results with other studies should be provided, and the possible reasons for these should be discussed based on the literature. For Results and Discussion, the contribution and importance of the results to science should be emphasized. The obtained results should be interpreted, avoiding unnecessary repetitions.

3.1. Structure Details and Analysis

In chemical computation, geometry optimization is a crucial procedure. Finding the minimal energy conformers at which all other attributes are acquired for conformationally flexible molecules requires a conformational search. Foresman and Frisch state that geometric parameters like bond length and bond angle may be effectively assessed as long as the experimental value's bond length differs from the expected value by less than 0.01 and the variation in the bond length angle is less than 1-2° [19]. Atomic attributes, including electronegativity, bond energy, and atomic size, are all determined by the length of the bond. Conversely, bond energy and electronegativity are equal to bond distance. With the DGDZVP and 6-311G(d,p) basis sets, the MP2 technique was used to compare BHDH molecule's bond lengths and angles [20].

Table 1 lists the optimized characteristics of the molecule, including the bond length between atoms, dihedral angles, and bond angles. When these two different basis sets are compared, the bond between the C-C atom for the DGDZVP basis set varied between 1.40Å-1.46Å, while the bond between the C-C atom for the 6-311G(d,p) basis set varied between 1.42Å-1.48Å. For both basis sets, the bond between C-C atoms showed close values. Bond angles and all bond lengths in phenyl rings are within the normal range. C-H bond lengths in the aromatic ring varied between 1.08-1.090Å. The distance between C23-Br26, C1-N2, and N2-N3 atoms has changed between 1.9032Å-1.9694Å, 1.3347Å-1.3631Å, and 1.4241Å-1.5222Å, respectively. All C-C-C angles for both basis sets are between 112° and 122°. The bond angle of C1-N2-N3 in the compound is 107.645°-109.018°, C5-N18-N19 is 119.677°-120.440°, and C22-C23-Br26 is 119.534°-119632°. We observed that the dihedral angles of the molecule are compatible with each other for both basis sets. We saw that the obtained theoretical bond lengths were close to the experimental numerical data in the literature [21, 22].

Table 1. BHDH molecules theoretically computed some bond lengths (Å) and bond angles (°)

Bond Lengths	MP2 DGDZVP	MP2 6-311G(d,p)	Bond Lengths	MP2 DGDZVP	MP2 6-311G(d,p)
C1-C5	1.45607	1.48908	**C23-Br26**	1.90326	1.96941
C4-C7	1.46574	1.48363	**C5-N18**	1.33650	1.35145
C8-C9	1.40394	1.42236	**N2-N3**	1.42417	1.52221
C7-C13	1.41334	1.43248	**C1-N2**	1.33474	1.36311
C15-C16	1.40574	1.42472	**N3-C4**	1.33227	1.35902
C7-C17	1.41349	1.43205	**N19-C20**	1.40973	1.43087
C1-C6	1.47190	1.48954	**N19-H37**	1.03005	1.02721
C20-C25	1.41334	1.42403	**C17-H36**	1.08954	1.09245
C20-C21	1.40786	1.42593	**C12-H31**	1.09348	1.09688
C24-C25	1.40226	1.42154	**C24-H40**	1.08946	1.09246
C1-C5-C4	103.34091	103.97700	**N18-N19-C20**	120.71695	119.87856
C4-C7-C17	121.27805	121.12912	**N18-N19-H37**	120.84485	121.06601
C1-N2-N3	109.01830	107.64582	**C7-C4-N3**	122.40228	121.97692
C5-N18-N19	119.67752	120.44011	**C20-C21-C22**	119.30439	119.34826
C22-C23-Br26	119.53433	119.63225	**C20-N19-H37**	118.43199	119.05126
C5-C4-C7-C13	149.85934	148.61603	**N18-C5-C4-N3**	166.71326	168.21426
N3-C4-C5-N18	166.71326	168.21426	**C21-C20-N19-H37**	177.21979	175.67830
C21-C22-C23-Br26	179.97135	179.91207	**C22-C23-C24-H40**	179.80592	179.84972
C5-N18-N19-C20	178.16709	177.98597	**C7-C4-N3-N2**	178.89941	178.63592

3.2. Mulliken Atomic Charges

Mulliken charges are present in the surrounding electron density, or charge density. It is helpful since it is susceptible to probability density and only depends on the base set [23]. Several MP2 approaches are used in Mulliken population studies to quantify the nuclear charges on atoms [24]. The MP2 technique and the basis set for DGDZVP and 6-311G(d,p) were used in its execution. Table 2 lists the Mulliken atomic charges. We observed either positive or negative Mulliken atomic charge values on carbon atoms. Every hydrogen atom had a positive net charge. When we look at the DGDZVP basic set values in Table 2, we observed that the electronegative atoms N2 (-0.234), N3 (-0.291), N18 (-0.121), and N19 (-0.606) had negative values. These atoms serve as acceptor atoms. When we examined both basis sets, we observed close values with negative values of Br26 -0.149 and -0.069. Additionally, graphical representations of the comparison of Mulliken charges of the BHDH molecule using two different base sets have been shown in Figure 1. When the Mulliken loads were compared in the two basic sets, we saw that the values were compatible.

Table 2. BHDH molecule's Mulliken atomic charges

ATOMS	MP2 / DGDZVP	MP2 / 6-311G(d,p)	ATOMS	MP2 / DGDZVP	MP2 / 6-311G(d,p)
C1	0.179	0.124	**N3**	-0.291	-0.244
C4	0.217	0.161	**N18**	-0.121	0.024
C6	0.051	0.240	**N19**	-0.606	-0.657
C7	0.120	0.260	**Br26**	-0.149	-0.069
C9	-0.242	-0.215	**H27**	0.268	0.246
C11	-0.245	-0.220	**H28**	0.347	0.218
C13	-0.275	-0.297	**H29**	0.249	0.221
C15	-0.241	-0.210	**H30**	0.245	0.217
C17	-0.288	-0.293	**H32**	0.276	0.251
C20	0.506	0.540	**H33**	0.239	0.212
C21	-0.338	-0.307	**H34**	0.240	0.213
C22	-0.216	-0.107	**H35**	0.233	0.207
C23	0.039	-0.345	**H37**	0.505	0.426
C24	-0.225	-0.107	**H38**	0.291	0.270
C25	-0.383	-0.375	**H39**	0.266	0.237
N2	-0.234	-0.189	**H41**	0.247	0.224

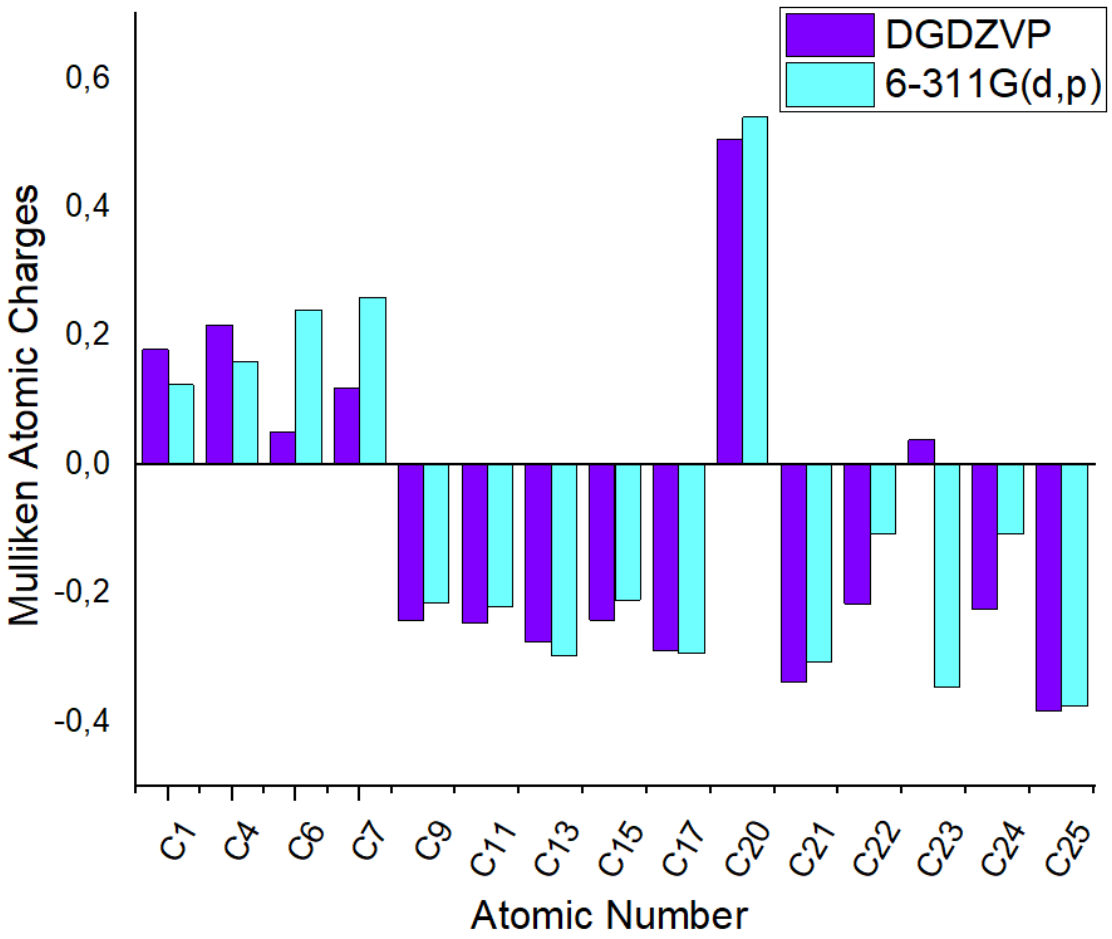

Figure 1. Mulliken atomic charge comparison for BHDH molecule

3.3. HUMO and LUMO Analysis

Molecules with soft expression, poor kinetic stability, and strong chemical reactivity are typically linked to their frontier orbital space. The molecule's relationships with other molecules are identified by its Highest-Energy Molecular Orbital (HOMO) and Lowest-Energy Molecular Orbital (LUMO) orbitals [25]. Band gap energies are computed, and HOMO-LUMO is predicted utilizing a solvation technique for a range of polar (water, DMSO, and ethanol) and non-polar (benzene) solvents. In advanced molecular orbital computation, the terms lowest unoccupied molecular orbital (LUMO) and highest occupied molecular orbital, HOMO, are recognized as significant FMO (frontier molecular orbital) orbitals [26]. Electrons in HOMO orbitals absorb high-frequency radiation, which causes them to leap into LUMO orbitals. Energies have a role in determining how sensitive Frontier Molecular Orbitals are overall to several descriptors, including electronegativity, global softness, electron affinity, global hardness, and chemical potential, as well as the molecule's global electrophilicity index [27]. The HOMO and LUMO orbital representations' of the densities of the BHDH molecule have been shown in Figures 2 and 3. As seen in Table 3, LUMO and HOMO for the DGD2VP set were calculated as -8.3535 eV and -0.1235 eV, respectively, while for the 311G(d,p) set, HOMO and LUMO were calculated as -8.4155 eV and -0.3671 eV, respectively. For the other orbitals of the DGD2VP set, $HOMO^{-1}$ and $LUMO^{+1}$ were calculated as -8.5399 eV and 2.2938 eV, respectively, while for the different orbitals of the 311G(d,p) set, $LUMO^{+1}$ and $HOMO^{-1}$ have been calculated as -8.2289 eV and 2.6313 eV, respectively. When we examine the two essential chemical orbitals for LUMO and HOMO energies in Figures 2 and 3, the HOMO and LUMO electron clouds are completely localized along the compound's ligand, as can be shown.

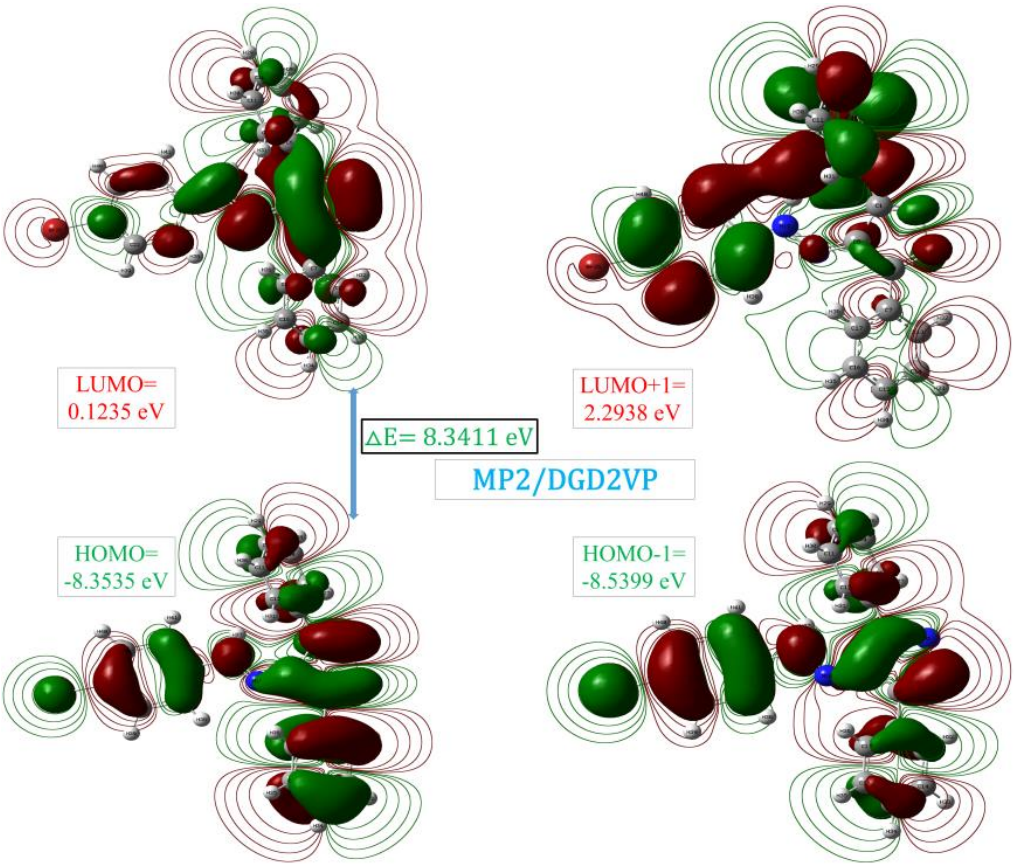

Figure 2. BHDH molecule's boundary molecular orbitals computed with the DGD2VP basic set

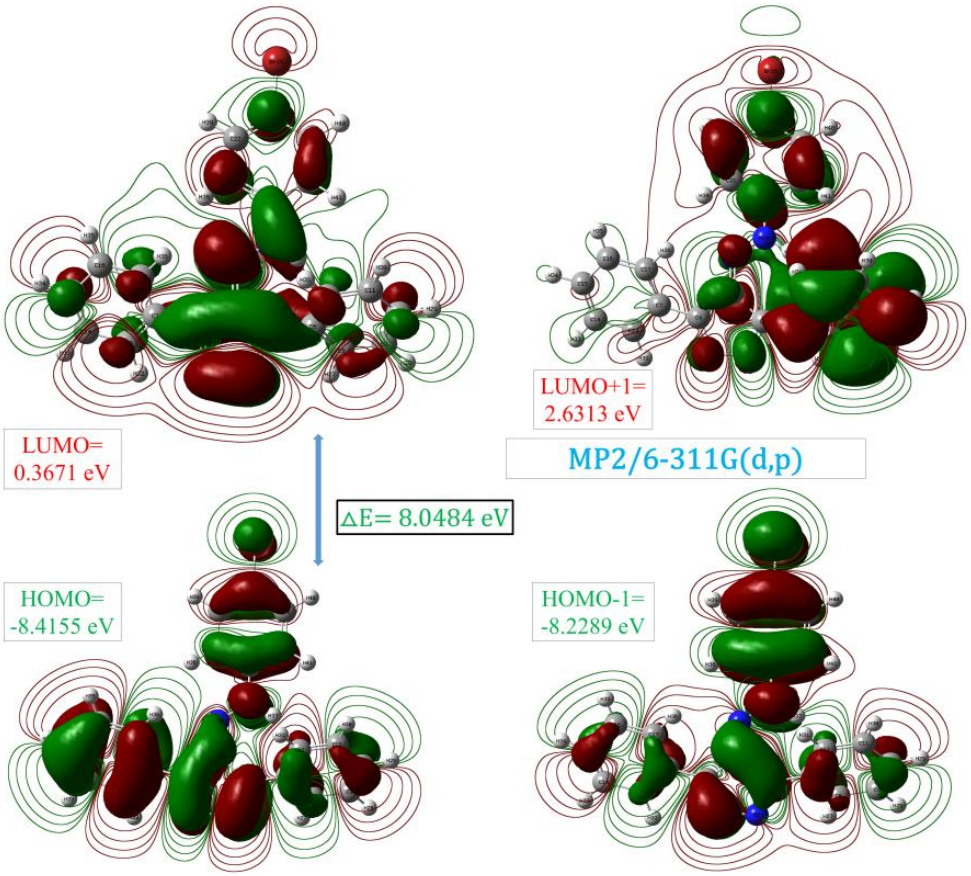

Figure 3. BHDH molecule's boundary molecular orbitals computed with the 6-311G (d,p) basic set

Table 3. Quantum chemical characteristics of the BHDH molecule computed utilizing the MP2/DGDZVP-MP2/6-311G techniques

Molecules Energy		MP2/DGD2VP	MP2/6-311G(d,p)
E_{LUMO}		0.1235	0.3671
E_{HOMO}		-8.3535	-8.4155
E_{LUMO+1}		2.2938	2.6313
E_{HOMO-1}		-8.5399	-8.2289
Energy Gap	$(\Delta E)\lvert E_{HOMO}-E_{LUMO}\rvert$	-8.477	-8.7826
Ionization Potential	$(I=-E_{HOMO})$	8.3535	8.4155
Electron Affinity	$(A=-E_{LUMO})$	-0.1235	-0.3671
Chemical hardness	$(\eta=(I-A)/2)$	8.477	8.7826
Chemical softness	$(s=I/2\eta)$	4.2385	4.3913
Chemical Potential	$(\mu=-(I+A)/2)$	-4.115	-4.0242
Electronegativity	$(\chi=(1+A)/2)$	8.23	8.0484
Electrophilicity index	$(\omega=\mu^2/2\eta)$	71.7715	71.41135

3.4. Molecular Electrostatic Potential (MEP)

The relative reactivity sites to nucleophilic and electrophilic attacks in a species are estimated using the molecular electrostatic potential, or MEP. Understanding nucleophilic (positive) and electrophilic (negative) locations for hydrogen bond interactions and chemical reactions depends on MEP surface analysis [28]. MEP displays the molecule size, shape, and electrostatic potential in point color order [29]. Different MEP values correspond to different hues. Maximum positive electrostatic potential is represented by the blue zone, zero potential by the green region, and maximum negative electrostatic potential by the red region. MEP accelerates the blue>green>red>orange process. Negative MEP seems to hold onto a proton depending on the electron density's evaluation within the molecule, while positive MEP detects protons repelled by their blue color (atomic nuclei) [30]. Figure 4 displays the MEP map of the compound BHDH using the MP2 technique with the basis sets DGDZVP and 6-311G(d,p). The MEP map displays positive and negative potential based on the measured data, clearly indicating the biological activity of BHDH. As expected, the negative sites were localized to the nitrogen in the pyrazole ring.

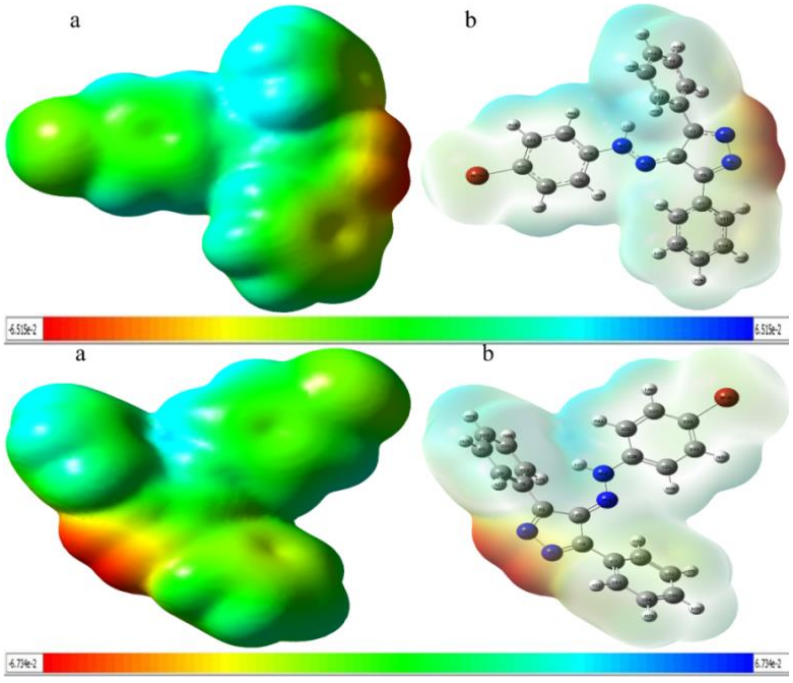

Figure 4. BHDH molecule's MEP surface calculated DGDZVP and 6-311G(d,p) basis sets

3.5. Nonlinear Optical Properties

When electromagnetic fields interact in disparate contexts, they produce new fields with distinct points, repetition, proficiency, and other characteristics from the dividing fields. This phenomenon is known as the Nonlinear Optical (NLO) effect [31]. π-conjugated particles and polymers are perfect for discovering these applications because of their ultrafast reactions and remarkable nonlinear characteristics. The blends of NLO materials show promise for all-optical interchange, recording, and restraint devices, even though they are not as promising for use in rapid electro-optical modulators and switches [32]. (3.1)-(3.3) demonstrate that the first-order hyperpolarizability of β, the second dipole moment μ, is the total first static hyperpolarizability of the x, y, and z components using the DGDZVP and 6-311G(d,p) basis sets with the MP2 technique and Using the restricted field technique, the polarizability α was found. Table 4 presents the μ, α, and β recorded for the studied atoms. The total values determined by the MP2 method using DGDZVP and 6-311G(d,p) basis sets to the DHPM compound are $2.77x10^{-30}$ esu and $2.70x10^{-30}$ esu, respectively.

$$\mu = (\mu_x^2 + \mu_z^2)^{\frac{1}{2}} \tag{3.1}$$

$$\beta_{Total} = (\beta^2 x + \beta^2 y + \beta^2 z)^{\frac{1}{2}} \tag{3.2}$$

and

$$\beta_{Total} = [(\beta xxx + \beta xyy + \beta xzz)^2 + (\beta yyy + \beta yxx + yzz)^2 + (\beta zzz + \beta zxx + \beta zyy)^2]^{\frac{1}{2}} \tag{3.3}$$

Table 4. NLO parameters of BHDH molecule computed using DGDZVP and 6-311G(d,p) basis sets with MP2 method

Parameters	MP2/DGD2VP	MP2/6-311G(d,p)	Parameters	MP2/DGD2VP	MP2/6-311G(d,p)
μ x	-4.2394	-2.9822	**β XXX**	-329.0799	-244.5529
μ y	1.8038	0.5759	**β YYY**	-0.7758	-12.5027
μ z	0.3618	0.4898	**β ZZZ**	-4.4802	-13.4906
μ (D)	4.6214	3.0765	**β XYY**	-52.8030	-6.8949
α XX	-206.8374	-183.9689	**β XXY**	-41.0396	-35.9322
α YY	-136.2896	-137.6760	**β XXZ**	-35.0058	13.0767
α ZZ	-168.1933	-170.7588	**β XZZ**	-54.4855	-87.1807
α XY	-9.4492	-9.3979	**β YZZ**	6.9026	-10.8462
α XZ	-6.5791	-2.6943	**β YYZ**	-16.2187	4.9378
α YZ	-1.1804	3.4442	**β XYZ**	-2.0695	-16.8616
α (au)	-175.172	-169.8441	**β (esu)**	$2.77x10^{-30}$	$2.70x10^{-30}$

3.6. NBO Analysis

The Natural Bond Orbital (NBO) study demonstrates increased conjugation, rearrangement, and intramolecular charge transfer of electrons in diverse orbitals. Research on natural bond orbitals sheds light on a compound's intra- and intermolecular hydrogen bonding and conjugative and hyper-conjugative interactions [33, 34]. The donor-acceptor stabilization energy E(2) related to delocalization i→j is computed as E(2)=qi for each donor NBO (i) and acceptor NBO (j). F(i,j)2/(εj−εi), where εi, εj are diagonal elements (orbital energies), and F(i,j) is the off-diagonal NBO Fock is the matrix element, and qi is the donor orbital occupancy. Because the stabilizing energy (E2) is larger, the conjugation across the molecular system is more extensive [35]. Table 5 presents the NBO analysis findings from the BHDH molecule utilizing the 6-311G(d,p) basis set and the MP2 technique. When we examine the results in Table 5, in the instance of C20/C25 benzene ring, πC20-C24 with π*C21-C22 (17.98 kcal/mol), πC21-C22 with π*C20-C25 (22.66 kcal/mol), πC23-C25 with π*C21-C22 (20.99 kcal/mol), and σC24-C25 and σ*C23-Br26 (22.66 kcal/mol) have high interaction energies. The molecule's intramolecular charge transfer and stability of the benzene rings under study are mostly due to

previously discussed stabilization energies. These energies stabilized the investigated molecule's structure, and an aromatic ring resonance interaction occurred between the heteroatoms. Additionally, the BHDH molecule has πC8-C9→π*C6-C12 (22.04 kcal/mol), πC15-C16→π*C7-C17 (21.27 kcal/mol), and πC10-C11→π*C6-C12 (21.05 kcal/mol). The other highest stabilization energies include πC6-C12→π*C10-C11 (20.74 kcal/mol) and πC7-C17→π*C13-C14 (19.38 kcal/mol). Consequently, the donor-acceptor interaction could be stabilized by electron delocalization between non-Lewis-type natural bond orbitals and unoccupied occupied Lewis. Further delocalization within the molecular system is seen from the electron density of double bonds and the conjugated single in the conjugated system. This leads to intramolecular charge transfer (ICT), stabilizing the system. These interactions weaken the corresponding bonds in the C-C antibonding orbital, manifesting as an increase in electron density (ED). Table 5 shows the significant stabilization energy of 22.66 kJ/mol and provides evidence for intramolecular charge transfer from (C21-C22) to *(C20-C25) antibonding orbitals. Also, the charge distribution of all hydrogen atoms is the same.

Table 5. Selected NBO results of BHDH molecule computed using DGDZVP and 6-311G(d,p) basis sets

NBO(i)	Type	Occupancies	NBO(j)	Type	Occupancies	E(2)[a] (Kcal/mol)	E (j)-E(i)[b] (a.u.)	F (i, j)[c] (a.u)
C1-N2	σ	1.98091	**C5-N18**	σ*	0.01944	4.44	1.25	0.067
C1-N2	π	1.88422	**C5-N18**	π*	0.32111	16.07	0.27	0.062
C1-C5	σ	1.97259	**C4-C7**	σ*	0.03186	5.45	1.12	0.070
N3-C4	π	1.88279	**C5-N18**	π*	0.32111	13.91	0.26	0.057
N2-N3	σ	1.96621	**C4-C7**	σ*	0.03186	6.04	1.10	0.073
C4-C5	σ	1.95989	**C1-C6**	σ*	0.03285	5.99	1.08	0.072
C4-C5	σ	1.95989	**N18-N19**	σ*	0.02382	6.32	0.96	0.070
C5-N18	π	1.80320	**N3-C4**	π*	0.24950	14.30	0.35	0.064
C6-C12	π	1.65932	**C10-C11**	π*	0.32831	20.74	0.28	0.068
C7-C17	π	1.62775	**C13-C14**	π*	0.29730	19.38	0.28	0.067
C8-C9	σ	1.98000	**C1-C6**	σ*	0.03285	4.53	1.12	0.064
C8-C9	π	1.64005	**C6-C12**	π*	0.39361	22.04	0.26	0.068
C8-H27	σ	1.97715	**C6-C12**	σ*	0.02668	5.85	1.00	0.068
C9-H28	σ	1.97757	**C10-C11**	σ*	0.01544	4.77	1.02	0.063
C10-C11	π	1.64875	**C6-C12**	π*	0.39361	21.05	0.27	0.067
C10-H29	σ	1.97848	**C11-C12**	σ*	0.01486	4.86	1.03	0.063
C11-H30	σ	1.97771	**C6-C12**	σ*	0.02668	5.27	1.03	0.065
C13-C14	π	1.65560	**C7-C17**	π*	0.37611	20.41	0.27	0.067
C13-H32	σ	1.97710	**C7-C17**	σ*	0.02402	5.59	1.01	0.067
C14-H33	σ	1.97777	**C15-C16**	σ*	0.01559	4.69	1.03	0.062
C15-C16	π	1.65498	**C7-C17**	π*	0.37611	21.27	0.27	0.069
C15-H34	σ	1.97883	**C13-C14**	σ*	0.01382	4.71	1.04	0.063
C16-C17	σ	1.97960	**C4-C7**	σ*	0.03186	4.48	1.12	0.064
C16-H35	σ	1.97787	**C7-C17**	σ*	0.02402	5.17	1.02	0.065
C20-C25	π	1.64550	**C21-C22**	π*	0.30596	17.98	0.29	0.065
C21-C22	π	1.67199	**C20-C25**	π*	0.40257	22.66	0.26	0.070
C23-C24	π	1.68181	**C21-C22**	π*	0.30596	20.99	0.29	0.070
C24-C25	σ	1.96833	**C23-Br26**	σ*	0.04044	5.21	0.76	0.056

3.7. ADME Analysis

One of its shared objectives is predicting Absorbed, Distributed, Metabolized, and Excreted (ADME) boundaries from subatomic structures. Lipinski and colleagues' landmark study looked at complicated combinations supplied orally to categorize physicochemical probes based on how likely they were to become oral drugs (drug-likeness) [36]. This illustrates the connection between pharmacokinetic and physicochemical limitations and is also known as the Rule of Five. The fivefold Lipinski standard meets roughly 91% of the ADME criteria. The standard explicitly addresses drug penetration through mixing-free drug distribution

within cell films. Special instances of this norm include tranquilizers that are effectively transported across cell layers by transporter proteins [37]. In the analysis conducted on ADME, Admetlab 2.0 (https://admetmesh.scbdd.com/), a free web tool for assessing drug similarity, was evaluated. This study investigated the drug-likeness of the BHDH molecule and ADME. Table 6 presents the estimated findings and interpretations of the investigated compound's physicochemical and lipophilicity features. Additionally, the medicinal chemistry applicability and comments of the compound are given in Table 7. Table 7 illustrates compliance with 49.11<140 (Topological Polar Surface Area) requirements for Lipinski's MW 402.05g/mol (<500), lipophilicity coefficient LogP 5.361 (≤ 5), H-acceptor 4 (≤ 12), H-bond donor 1 (<7). The color zones and physicochemical parameters map of the studied compound are given in Figure 5. The outcomes demonstrated no breach of Lipinski's five rules, indicating how drug-like the molecule is. Because of the compound's promising permeability, lipophilicity, and solubility, it demonstrated excellent absorption. The polar surface region and the quantity of rotatable bonds showed the investigated compound's high bioavailability.

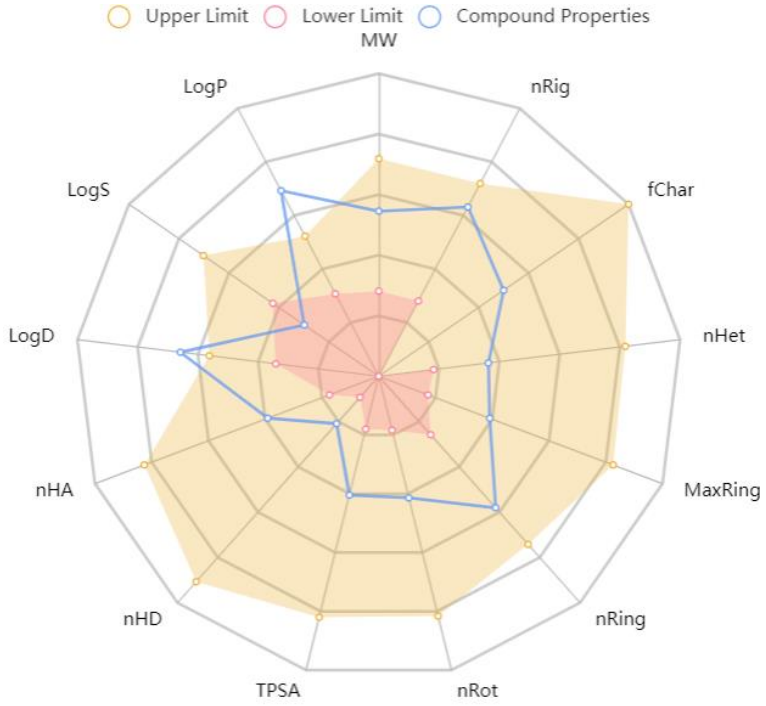

Figure 5. Color regions and physicochemical parameters of BHDH molecule

Table 6. Physicochemical and lipophilicity of BHDH molecule

Property	Value	Comment
Molecular Weight	402.05	Contain hydrogen atoms. Optimal:100~600
nHA	4	Number of hydrogen bond acceptors. Optimal:0~12
nHD	1	Number of hydrogen bond donors. Optimal:0~7
nRot	4	Number of rotatable bonds. Optimal:0~11
nRing	4	Number of rings. Optimal:0~6
MaxRing	6	Number of atoms in the biggest ring. Optimal:0~18
nHet	5	Number of heteroatoms. Optimal:1~15
nRig	24	Number of rigid bonds. Optimal:0~30
TPSA	49.11	Topological Polar Surface Area. Optimal:0~140
logS	-6.038	Log of the aqueous solubility. Optimal: -4~0.5 log mol/L
logP	5.361	Log of the octanol/water partition coefficient. Optimal: 0~5

Table 7. Medicinal chemistry of BHDH molecule

Property	Value	Decision	Comment
QED	0.604	-	A measure of drug-likeness based on the conceptof desirability; Attractive: > 0.67; unattractive: 0.49~0.67; toocomplex: < 0.34
Fsp3	0.0	-	$Fsp^3 \geq 0.42$ is considered a suitable value.
MCE-18	38.0	-	MCE-18 stands for medicinal chemistry evolution.MCE-18≥45 is considered a suitable value.
LipinskiRule	Accepted	-	MW ≤ 500; logP ≤ 5; Hacc ≤10; Hdon ≤ 5 If two properties are out of range, a poor absorption or permeability is possible; one isacceptable.
Pfizer Rule	Rejected	-	logP > 3; TPSA < 75Compounds with a high log P (>3) and low TPSA(<75) are likely to be toxic.
Golden Triangle	Accepted	-	200 ≤ MW ≤ 50; -2 ≤ logD ≤ 5 Compounds satisfying the Golden Triangle rulemay have a more favorable ADMET profile.
PAINS	0 alerts	-	Pan Assay Interference Compounds, frequent hitters, Alpha-screen artifacts, and reactive compound
ALARMNMR	2 alerts	-	Thiol reactive compounds
BMS	0 alerts	-	Reactive compounds, Undesirable
ChelatorRule	0 alerts	-	Chelating compounds

3.8. Molecular Docking Studies

All functions and activities in any living system, human, animal, plant, fungal, or bacterial, can be converted into biological processes at the molecular, cellular, or organ level. Molecular docking is a crucial method in medication design based on a structure that can help expedite and simplify the new medication creation process [38]. Molecular docking estimates any species' binding conformations and affinities to the goal protein, enabling scientists to digitally scan the interaction between the protein and the ligand [39]. By providing predictions for the bound shape of the ligand and a way to energetically rank the protein-ligand interaction, molecular docking techniques aid in the characterization of the protein-ligand interaction [40]. Molecular docking was done using Schrödinger's Maestro Molecular Modeling platform to analyze the ligand-protein interactions of the BHDH molecule with acetylcholinesterase (AChE) and butyrylcholinesterase (BChE) enzymes on obesity disease [17]. Acetylcholinesterase (AChE) (PDB: 1ACJ) and butyrylcholinesterase (BChE) (PDB: 1P0I) enzymes required for docking were searched from the online resource RSCB protein database. Using the Discovery Studio Client 2017 program, good docking poses were chosen for the docking analysis on obesity illness, and the protein-ligand interaction was shown [18]. Protein binding and active sites are often anchored in structured cavities and pockets. In order to prevent steric hindrance, water molecules were eliminated from the crystal packing. Excellent enzyme binding affinity was attained: -9.73 kcal for BChE and -10.00 kcal for AChE. The binding energy value affects the target protein's choice of ligand docking. Each species has a stronger capacity to attach to the target protein, the more negatively its binding energy value is. Given the high binding affinity of the BHDH molecule, we believe that the chemical we studied will be crucial to creating medications based on structure to treat obesity. The docking scores of these enzymes are given in Table 8. Visualized findings of the BHDH molecule and the ligands' interactions and separations have been given in Figures 6 and 7. Additionally, essential interactions, amino acids, and bond length data of our study compound in the docking analysis are given in Tables 9 and 10.

Table 8. Docking score of BHDH molecule PDB: 1ACJ and PDB: 1P0İ

Compound	Docking Score	
	(PDB: 1ACJ)	(PDB: 1P0İ)
BHDH Molecule	-10.00	-9.73

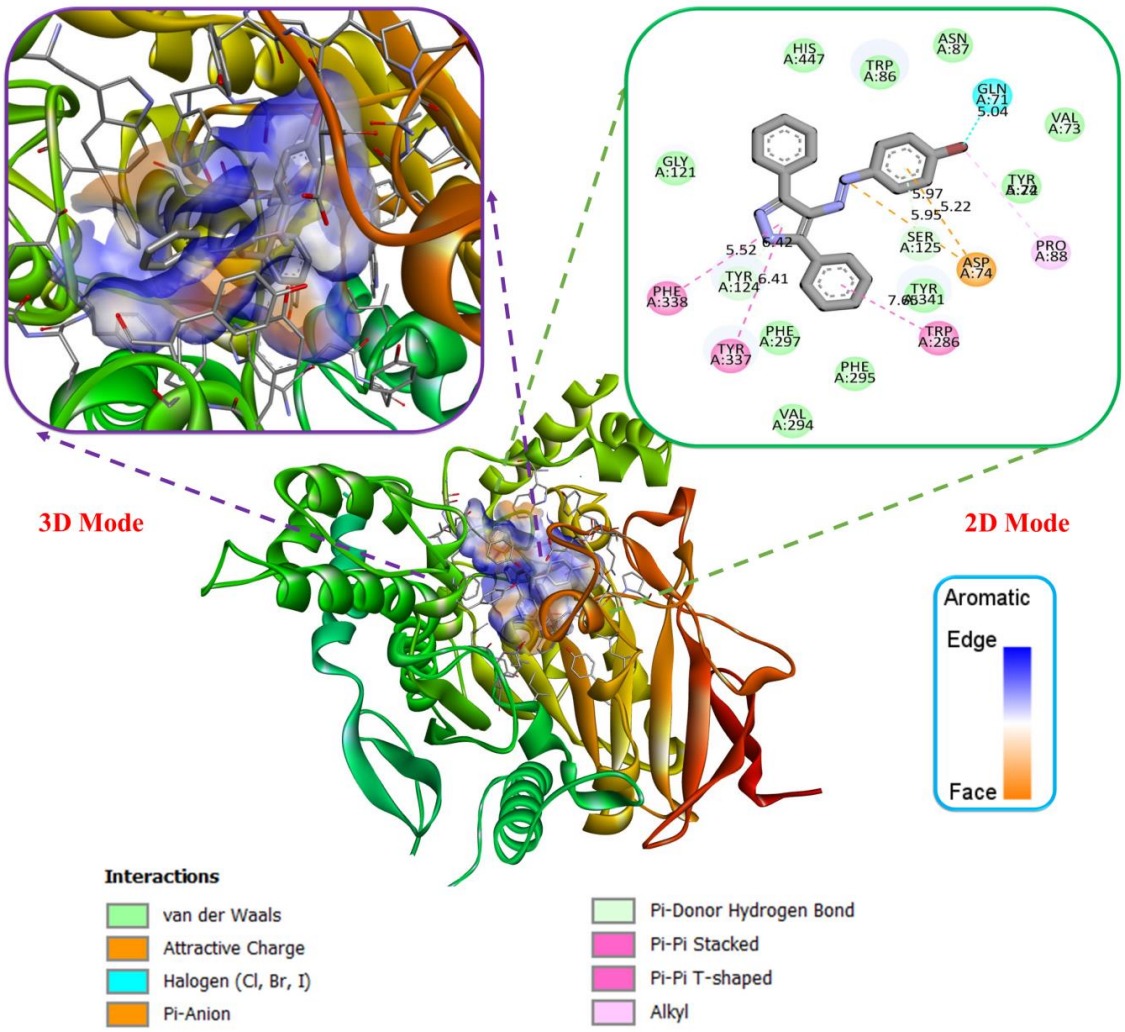

Figure 6. 3D and 2D representations of the interaction between BHDH compound of AChE enzyme

Table 9. Parameters of the interaction between BHDH compound of AChE enzyme

Important Interactions	Full Name	Type	Bond Length (Å)	Color
Attractive Charge	A:ASP74	AsparticAcid	5.95	
Halojen	A:GLN71	Glutamine	-	
Pİ-Pi Stacked	A:TRP286	Tryptophan	7.65	
Pi-Pi T-shaped	A:TYR337	Tyrosine	6.41	
	A:PHE338	Phenylalanine	5.52	
Alkyl	A:PRO88	Proline	5.74	
Pi-Anion	A:ASP74	AsparticAcid	5.22	
Pi-donor Hydrogen Bond	A:SER125	Serine	5.97	
Van der Waals	A:VAL73 A:ASN87	Valine Asparagine	- -	

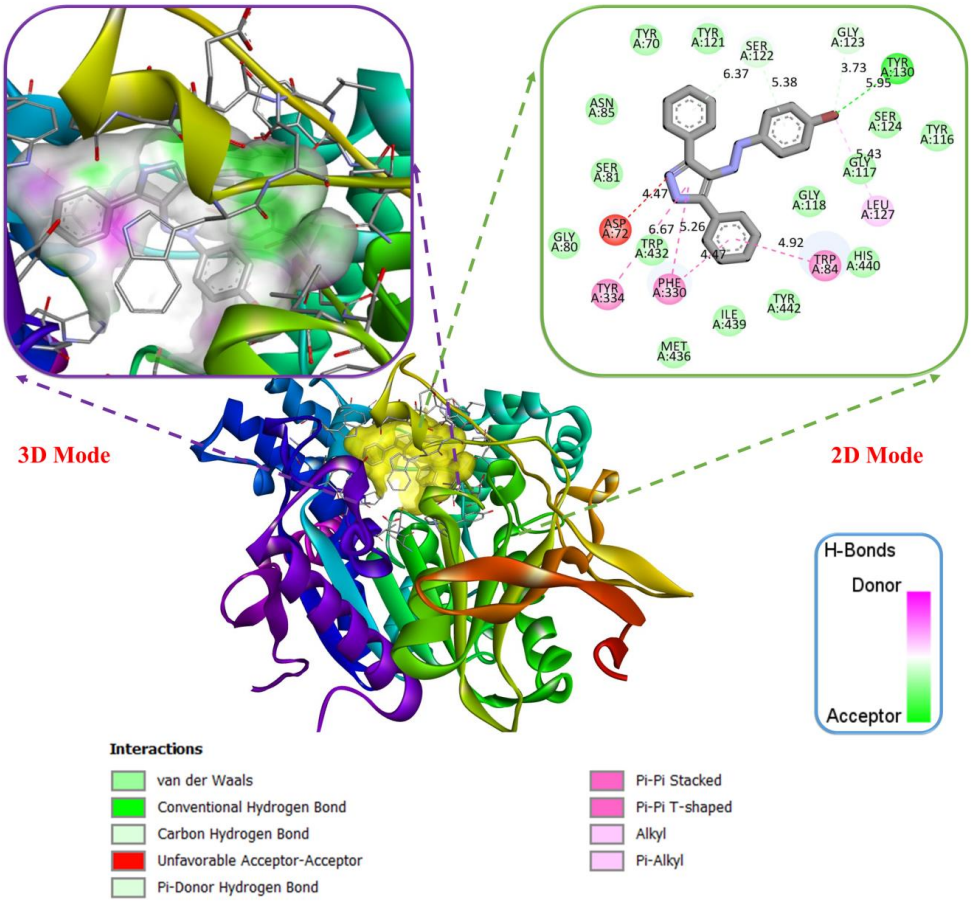

Figure 7. 3D and 2D representations of the interaction between BHDH compound of BChE enzyme

Table 10. Parameters of the interaction between BHDH compound of BChE enzyme

Important Interactions	Full Name	Type	Bond Length (Å)	Color
Conventional Hydrogen Bond	A:TYR130	Tyrosine	5.95	
Unfavorable Acceptor-acceptor	A:ASP72	AsparticAcid	4.47	
Pİ-Pi Stacked	A:TRP84	Tryptophan	4.94	
	A:PHE330	Phenylalanine	5.26, 4.47	
Pi-Pi T-shaped	A:TYR334	Tyrosine	6.67	
Pi-Alkyl	A:LEU127	Leucine	5.43	
Carbon Hydrogen Bond	A:GLY123	Glycine	3.73	
Pi-donor Hydrogen Bond	A:SER122	Serine	5.38, 6.37	
Van der Waals	A:SER81	Serine	-	
	A:MET436	Methionine	-	

4. Conclusion

This study, quantum chemical calculations were made for the 4-(2-(4-bromophenyl)hydrazineylidene)-3,5-diphenyl-4h-pyrazole (BHDH) molecule using the MP2 method and DGDZVP and 6-311G(d,p) basis sets. These two basis sets have computed structural parameters (bond lengths, bond angles, and dihedral angles). We found that the structural parameters calculated with these basis sets are compatible. NLO, HOMO-LUMO,

MEP, NBO, and Mulliken loadings were visualized using the same basis sets. The investigated chemical was suitable for use as an NLO material. From the calculations made for the BHDH molecule, polarity (α=-175.172 au and α=-169.8441 au) and static high-order polarity (β=2.77x10^{-30} esu and β=2.70x10^{-30} esu) parameters were determined. The boundary molecular energy gap between LUMO and HOMO calculations of the examined compound is -8.477 eV for the DGD2VP set and -8.7826 eV for the 6-311G(d,p) set; this indicates greater stability of the molecule. When we examined the MEP of our compound, the negative regions were localized to the nitrogen in the pyrazole ring, as we expected. When we compared the mulliken atomic charges in the two sets used, we observed the compatibility of the mulliken charges in the two sets. In the continuation of the study, ADME analysis was performed to evaluate the BHDH molecule as a drug. We discovered that the molecule had strong ADME qualities and met Lipinski's rule requirements, indicating that it is a viable therapeutic candidate that should be investigated further. Finally, our study analyzed the ligand-protein interactions of the BHDH molecule with AChE and BChE enzymes in obesity disease. Good binding affinity for the enzyme was obtained, with the binding affinity being -10.00 for AChE and -9.73 kcal for BChE. Since the BHDH molecule has good binding affinity, this study compound will be an essential prediction in structure-based drug design on obesity disease.

Author Contributions

All the authors equally contributed to this work. They all read and approved the final version of the paper.

Conflicts of Interest

All the authors declare no conflict of interest.

Ethical Review and Approval

No approval from the Board of Ethics is required.

References

[1] J. V. Faria, P. F. Vegi, A. G. C. Miguita, M. S. Dos Santos, N. Boechat, A. M. R. Bernardino*, Recently reported biological activities of pyrazole compounds*, Bioorganic and Medicinal Chemistry 25 (21) (2017) 5891–5903.

[2] A. M. Youssef, E. G. Neeland, E. B. Villanueva, M. S. White, I. M. El-Ashmawy, B. Patrick, A. Klegeris, A. S. Abd–El–Aziz, *Synthesis and biological evaluation of novel pyrazole compounds,* Bioorganic and Medicinal Chemistry 18 (15) (2010) 5685–5696.

[3] H. Ma, S. Chen, Z. Liu, Y. Sun, *Theoretical elucidation on the inhibition mechanism of pyridine–pyrazole compound: A Hartree Fock study,* Journal of Molecular Structure: THEOCHEM 774 (1-3) (2006) 19–22.

[4] A. R. Thomas, Y. S. Mary, K. Resmi, B. Narayana, B. Sarojini, G. Vijayakumar, C. Van Alsenoy, *Two neoteric pyrazole compounds as potential anti-cancer agents: Synthesis, electronic structure, physico-chemical properties and docking analysis*, Journal of Molecular Structure (1181) (2019) 455–466.

[5] B. E. Levin, *Factors promoting and ameliorating the development of obesity*, Physiology and Behavior 86 (5) (2005) 633–639.

[6] R. Dent, R. McPherson, M. E. Harper, *Factors affecting weight loss variability in obesity,* Metabolism 113 (154388) (2020).

[7] B. E. Levin, *Developmental gene environment interactions affecting systems regulating energy homeostasis and obesity,* Frontiers in Neuroendocrinology 31 (3) (2010) 270–283.

[8] L. S. Adair, *Child and adolescent obesity: Epidemiology and developmental perspectives*, Physiology Behavior 94 (1) (2008) 8–16.

[9] I. Orhan, B. Şener, M. Choudhary, A. Khalid, *Acetylcholinesterase and butyrylcholinesterase inhibitory activity of some Turkish medicinal plants*, Journal of Ethnopharmacology 91 (1) (2004) 57–60.

[10] G. Chuiko, V. Podgornaya, Y. Zhelnin, *Acetylcholinesterase and butyrylcholinesterase activities in brain and plasma of freshwater teleosts: Cross–species and cross-family differences*, Comparative Biochemistry and Physiology Part B: Biochemistry and Molecular Biology 135 (1) (2003) 55–61.

[11] R. Scacchi, M. Ruggeri, R. M. Corbo, *Variation of the butyrylcholinesterase (BChE) and acetylcholinesterase (AChE) genes in coronary artery disease*, Clinica Chimica Acta 412 (15–16) (2011) 1341–1344.

[12] F-G. Koçanc, B. Aslım, *Structure and functions of acetylcholinesterase and acetylcholinesterase inhibitory activity of plants*, Manas Journal of Agriculture Veterinary and Life Sciences 6 (1) (2016) 19–35.

[13] O. Christiansen, *Møller–Plesset perturbation theory for vibrational wave functions*, The Journal of Chemical Physics 119 (12) (2003) 5773–5781.

[14] T. Takatani, C. D. Sherrill, *Performance of spin–component-scaled Møller–Plesset theory (SCS–MP2) for potential energy curves of noncovalent interactions*, Physical Chemistry Chemical Physics 9 (46) (2007) 6106–6114.

[15] F. Turkan, A. Cetin, P. Taslimi, İ. Gulçin, *Some pyrazoles derivatives: Potent carbonic anhydrase, α-glycosidase, and cholinesterase enzymes inhibitors*, Archiv der Pharmazie 351 (10) (2018) 1800200.

[16] T. J. Frisch, G. W. Trucks, H. B. Schlegel, G. E. Scuseria, M.A. Robb, J. R. Cheeseman, G. Scalmani, V. P. G. A. Barone, G. A. Petersson, H. J. R. Nakatsuji, Gaussian 16 Revision C.01. Gaussian Inc, Wallingford, Connecticut, 2016.

[17] S. Release, 1: Maestro, Schrodinger, LLC, New York, 2019.

[18] BIOVIA Discovery Studio D. SYSTÈMES BIOVIA Corporate Europe, BIOVIA 334 Cambridge Science Park Cambridge, 2016. http://accelrys.com/products/collaborativescience/biovia-discovery-studio.

[19] K. Gören, M. Bağlan, İ. Çakmak, *Theoretical investigation of 1H and 13C NMR spectra of diethanol amine dithiocarbamate RAFT agent*, Journal of the Institute of Science and Technology 12 (3) (2022) 1677–1689.

[20] K. Gören, Ü. Yıldıko, *Aldose reductase evaluation against diabetic complications using ADME and molecular docking studies and DFT calculations of spiroindoline derivative molecule*, Süleyman Demirel University Journal of Natural and Applied Sciences 28 (2) (2024) 281–292.

[21] R. Renjith, Y. S. Mary, C. Y. Panicker, H. T. Varghese, M. Pakosińska-Parys, C. Van Alsenoy, T. Manojkumar, *Spectroscopic (FT-IR, FT-Raman), first order hyperpolarizability, NBO analysis, HOMO and LUMO analysis of 1, 7, 8, 9-tetrachloro-10, 10-dimethoxy-4-[3-(4-phenylpiperazin-1-yl) propyl]-4-azatricyclo [5.2. 1.02, 6] dec-8-ene-3, 5-dione by density functional methods*, Spectrochimica Acta Part A: Molecular and Biomolecular Spectroscopy 124 (2014) 500–513.

[22] K. Gören, M. Bağlan, Ü. Yıldıko, *Melanoma cancer evaluation with ADME and molecular docking analysis, DFT calculations of (E)-methyl 3-(1-(4-methoxybenzyl)-2,3-dioxoindolin-5-yl)-acrylate molecule*, Journal of the Institute of Science and Technology 14 (3) (2024) 1186–1199.

[23] K. Gören, M. Bağlan, Ü. Yıldıko, V. Tahiroğlu, *Molecular docking and DFT analysis of thiazolidinone-bis Schiff base for anti-cancer and anti-urease activity*, Journal of the Institute of Science and Technology 14 (2) (2024) 822–834.

[24] M. Arivazhagan, V. Subhasini, R. Kavitha, R. Senthilkumar, *The spectroscopic (FT-IR, FT-Raman), MESP, first order hyperpolarizability, NBO analysis, HOMO and LUMO analysis of 1, 5-dimethyl napthalene by density functional method,* Spectrochimica Acta Part A: Molecular and Biomolecular Spectroscopy 131 (2014) 636–646.

[25] M. Suhasini, E. Sailatha, S. Gunasekaran, G. Ramkumaar, *Vibrational and electronic investigations, thermodynamic parameters, HOMO and LUMO analysis on Lornoxicam by density functional theory*, Journal of Molecular Structure 1100 (2015) 116–128.

[26] M. Bağlan, K. Gören, Ü. Yıldıko, *HOMO–LUMO, NBO, NLO, MEP analysis and molecular docking using DFT calculations in DFPA molecule*, International Journal of Chemistry and Technology 7 (1) (2023) 38–47.

[27] P. Demir, F. Akman, *Molecular structure, spectroscopic characterization, HOMO and LUMO analysis of PU and PCL grafted onto PEMA-co-PHEMA with DFT quantum chemical calculations*, Journal of Molecular Structure 1134 (2017) 404–415.

[28] M. Bağlan, Ü. Yıldıko, K. Gören, *Computational Investigation of 5.5'',7''-trihydroxy-3,7-dimethoxy-4'-4'''-O-biflavone from Flavonoids Using DFT Calculations and Molecular Docking*, Adıyaman University Journal of Science 12 (2) (2022) 283–298.

[29] M. Bağlan, K. Gören, Ü. Yıldıko, *DFT Computations and Molecular Docking Studies of 3-(6-(3-aminophenyl)thiazolo1,2,4triazol-2-yl)-2H-chromen-2-one (ATTC) Molecule*, Hittite Journal of Science and Engineering 10 (1) (2023) 11–19.

[30] M. Arivazhagan, V. Subhasini, R. Kavitha, R. Senthilkumar, *The spectroscopic (FT-IR, FT-Raman), MESP, first order hyperpolarizability, NBO analysis, HOMO and LUMO analysis of 1,5-dimethyl naphthalene by density functional method,* Spectrochimica Acta Part A: Molecular and Biomolecular Spectroscopy 131 (2014) 636–646.

[31] M. Bağlan, Ü. Yıldıko, K. Gören, *Dft Calculations And Molecular Docking Study In 6-(2-Pyrrolidinone-5-yl)-Epicatechin Molecule From Flavonoids*, Eskişehir Technical University Journal of Science and Technology B-Theoretical Sciences 11 (1) (2023) 43–55.

[32] A. Mahmood, S. U. D. Khan, U. A. Rana, M. R. S. A. Janjua, M. H. Tahir, M. F. Nazar, Y. Song, *Effect of thiophene rings on UV/visible spectra and nonlinear optical (NLO) properties of triphenylamine based dyes: A quantum chemical perspective*, Journal of Physical Organic Chemistry 28 (6) (2015) 418–422.

[33] E. Çimen, V. Tahiroğlu, *3-[1-(5-Amino-[1,3,4]tiadiazol-2-il)-2-(1H-imidazol-4-il)-etilimino]-2,3-dihidro-indol-2-on Theoretical Study of the Molecule*, Turkish Journal of Nature and Science 13 (2) (2024) 6–13.

[34] K. Gören, E. Çimen, V. Tahiroğlu, Ü. Yildiko, *Moleculer Docking and Theoretical Analysis of the (E)-5-((Z)-4-methylbenzylidene)-2-(((E)-4-methylbenzylidene)hydrazineylidene)-3-phenylthiazolidin-4-one Molecule*, Bitlis Eren University Journal of Science 13 (3) (2024) 659–672.

[35] M. Govindarajan, M. Karabacak, *Spectroscopic properties, NLO, HOMO–LUMO and NBO analysis of 2,5-Lutidine, Spectrochimica Acta Part A: Molecular and Biomolecular Spectroscopy* 96 (2012) 421–435.

[36] N. Lohit, A. K. Singh, A. Kumar, H. Singh, J. P. Yadav, K. Singh, P. Kumar, *Description and in silico ADME studies of US-FDA approved drugs or drugs under clinical trial which violate the Lipinski's rule of 5*, Letters in Drug Design Discovery 21 (8) (2024) 1334–1358.

[37] M. P. Gleeson, A. Hersey, S. Hannongbua, *In-silico ADME models: A general assessment of their utility in drug discovery applications,* Current Topics in Medicinal Chemistry 11 (4) (2011) 358–381.

[38] S. Yenigun, Y. Basar, Y. Ipek, L. Behcet, I. Demirtas, T. Özen, *Comprehensive evaluation of Ixoroside:*

An iridoid glycoside from Nepeta aristata and N. baytopii, assessing antioxidant, antimicrobial, enzyme inhibitory, DNA protective properties, with computational and pharmacokinetic analyses, Journal of Biologically Active Products from Nature 14 (3) (2024) 286–315.

[39] R. Riaz, S. Parveen, M. Rashid, N. Shafiq, *Combined experimental and theoretical insights: Spectroscopic and molecular investigation of polyphenols from fagonia indica via DFT, UV–vis, and FT-IR approaches*, ACS Omega 9 (1) (2023) 730–740.

[40] A. A. Tanrıverdi, K. Altun, Ü. Yıldıko, İ. Çakmak, *Structural and spectral properties of 4-(4-(1-(4-Hydroxyphenyl)-1-phenylethyl)phenoxy)phthalonitrile: Analysis by TD-DFT method, ADME analysis and docking studies*, International Journal of Chemistry and Technology 5 (2) (2021) 147–155.